IJCRT.ORG ISSN : 2320-2882

INTERNATIONAL JOURNAL OF CREATIVE RESEARCH THOUGHTS (IJCRT)

An International Open Access, Peer-reviewed, Refereed Journal

Investigation on room temperature ferromagnetic Fe doped NiO dilute magnetic semiconductor as a functional material for spintronics application

Narayan Das
Department of Physics, Arya Vidyapeeth College, Guwahati, India.

Abstract

In this research, the properties of Fe doped NiO systems are studied as the material dimensions are reduced to nanometer length scales. The samples are prepared by sintering the corresponding precursor in air at temperature 600°C. The synthesis was done by a chemical co-precipitation and post-thermal decomposition method. Polycrystalline monophase pure $Ni_{1-x}Fe_xO$ (x=0.04) have been obtained as evident from x-ray diffraction study. Higher concentration of Fe leads to the formation of different materials and phases like NiO, $NiFe_2O_4$, Fe_2O_3 etc. Microstructural analysis revealed the presence of monodispersed spherical particles of average size 12 nm and lattice strain 0.65. Magnetic measurements clearly reveal the ferromagnetic behaviour at room temperature. The semiconducting behaviour of the sample is ensured by performing conductivity study. The optical characterization is done for the sample to study the energy level characteristic.

Key words: DMS, nanoparticle, ferromagnetism, spintronics.

1. Introduction:

An approach compatible with the semiconductor used in present day electronics is to make nonmagnetic semiconductors magnetic, and even ferromagnetic by introducing a high concentration of magnetic ions. By combining the properties of magnetics with that of semiconductors, the novel class of materials, known as dilute magnetic semiconductors (DMSs), are considered a promising system for exhibiting spintronics functionality. A dilute magnetic semiconductor can be realized by alloying of magnetic elements in a regular semiconductor. An important consequence of this substitutional alloying is that the magnetic atoms are diluted and have a random distribution. The exchange interaction between the conduction carriers and the localized moments of the magnetic ions can alter the transport, optical and magnetic properties of the host semiconductor. To achieve room temperature ferromagnetism, which is the subject of intense research interest, we selected Fe doped NiO DMS system. NiO was choosen as the target material, because it has lattice and magnetic structural similarities to that of transition metal oxides. Bulk NiO has optical band gap of 4.0 eV and therefore is an insulator having conductivity of the order of 10^{-13} S/cm at room temperature[15]. The study of magnetic character of NiO shows that it is antiferromagnetic having T_N= 523 K[16]. But the same after doping with transition metal like Fe gain large magnetic moment at room temperature. The present miniaturization trend in science and technology demands the devices with minimal size but with higher efficiency and better performance. The reduction in size of this functional material will explore novel and interesting magnetic (spin) and semiconducting (charge) behaviour to add new era for spintronics technology. Taking into consideration these aspects, we discuss in this paper our results on the preparation, microstructural and physical properties of ultrafine Fe doped NiO particles.

2. Experimental Details

The synthesis of NiO:Fe nanoparticles by a chemical co-precipitation and post-thermal decomposition method was carried out under ambient air atmosphere. In this typical preparation method, $Ni(NO_3)_2.6H_2O$, $Fe(NO_3)_3.9H_2O$ and NH_4HCO_3 were used as starting raw materials. Highly pure $Ni(NO_3)_2.6H_2O$ and $Fe(NO_3)_3.9H_2O$ was dissolved in double distilled water. On the other hand, solution of NH_4HCO_3 was prepared with doubled distilled water as the solvent so that the pH of the solution becomes 8 at room temperature. Then, the NH_4HCO_3 solution was slowly added into the mixture of $Ni(NO_3)_2.6H_2O$ and $Fe(NO_3)_3.9H_2O$ which was continuously stirred. The resultant precipitate along with the mother solution was allowed to settle for around 24 hrs. Then the precipitation was centrifuged and filtered out. The so obtained sample was then washed several times with double distilled water and ethanol and then dried at 80 ^{0}C for around 24 hrs. Subsequently, the material was calcined in air at 600 ^{0}C for 4 hrs in a horizontal tube furnace with PID controller in open quartz tube under ambient air atmosphere to obtain the ultrafine powder of Fe doped NiO nanoparticles. TEM and XRD measurements were used for size, shape, distribution and phase analysis of the obtained nanoparticles. The PL was excited using a range of wavelengths 450-600 nm. The magnetic and electrical conductivity characteristics were investigated at room temperature.

3. Results and Discussion:

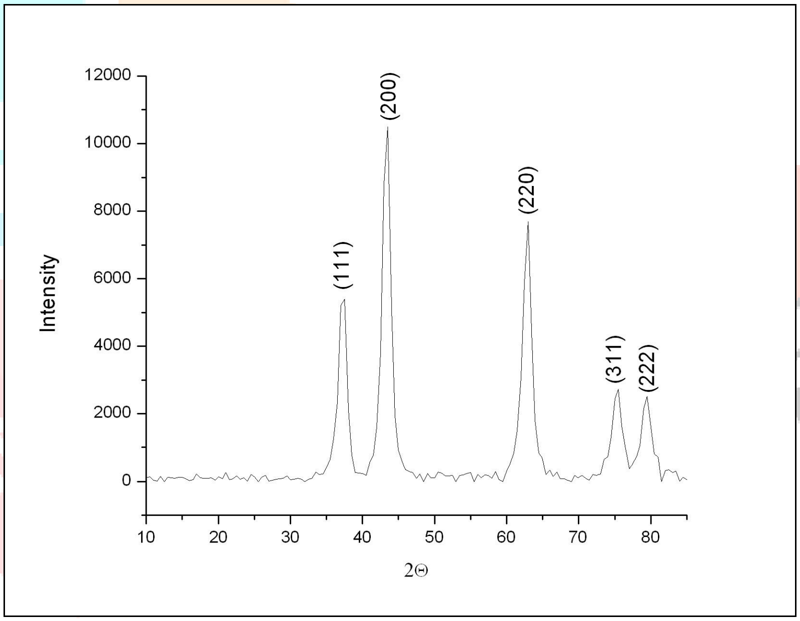

Figure 1 XRD pattern of Ni1-xFexO (x=0.04) sample (S1)

The XRD pattern of the so prepared sample is shown in Fig. 1. The careful analysis of the XRD pattern reveals the presence of $Ni_{1-x}Fe_xO$ (x=0.04) in the sample with five intense peaks of NiO. The five peaks in the pattern are very sharp and symmetric depicting the monophase polycrystalline existence of Fe doped NiO. The XRD pattern were then analysed based on a pattern decomposition procedure using a pseudo-Voigt profile shape function and subsequent single line analysis based on the equivalent Voigt presentation. The analysis provided the crystallite size and lattice strain. The structurally broadened profile was obtained by subtracting standard sample profile from experimentally broadened profile. The analyses were performed on individual peaks and the average crystallite size and lattice strain was noted. The average crystallite size was found to be 12 nm and the corresponding lattice strain was 0.651. The samples with higher concentration of Fe (x=0.05, 0.06, 0.07, 0.08 etc) were also examined through XRD analysis. It shows no change in the number of peaks and peak position. The XRD patterns of these samples show a slight increase in intensity and reduction in peak broadening with increase in Fe doping. It is due to growth of the crystal and lattice planes. Subsequently, we prepared a series of samples with higher doping concentrations. Here, we have shown the XRD characteristic of a sample with very high Fe doping concentration (x=0.2) (refer Fig. 2). Interestingly, the analysis shows the presence of several phases of NiO, Fe_2O_3 and their alloys. The experimental d_{hkl} values were compared with standard d_{hkl} values from JCPDS data file and the analysis confirms presence of $NiFe_2O_4$, Fe_2O_3, NiO etc. The samples with Fe doping concentration much less than x=0.04 are not showing the presence of prominent peaks in the XRD pattern. Hence, the Fe doped NiO nanoparticles with doping concentration x=0.04 was used for further study.

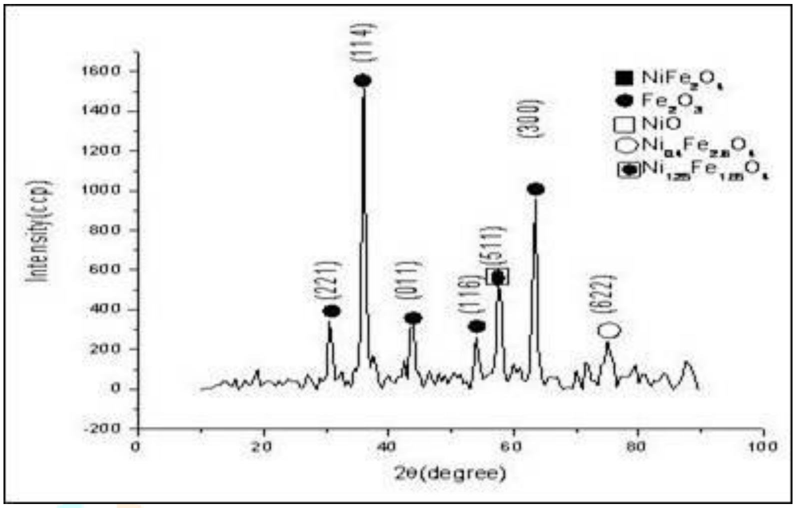

Figure 2 XRD pattern of Ni1-xFexO (x=0.2) sample (S2)

Fig. 3 shows the transmission electron micrograph (TEM) of the $Ni_{1-x}Fe_xO$ (x=0.04) sample. The TEM image shows the presence of spherical shaped particles with a uniform size distribution. The average particle size estimated from the image analysis is found to be 17 nm. The difference in the size measured from XRD and TEM analysis may be attributed to the formation of clusters. The elemental composition was studied by energy dispersive x-ray (EDX) analysis. The analysis shows the strong presence of Ni and O with trace amount of Fe. This result corroborates XRD findings.

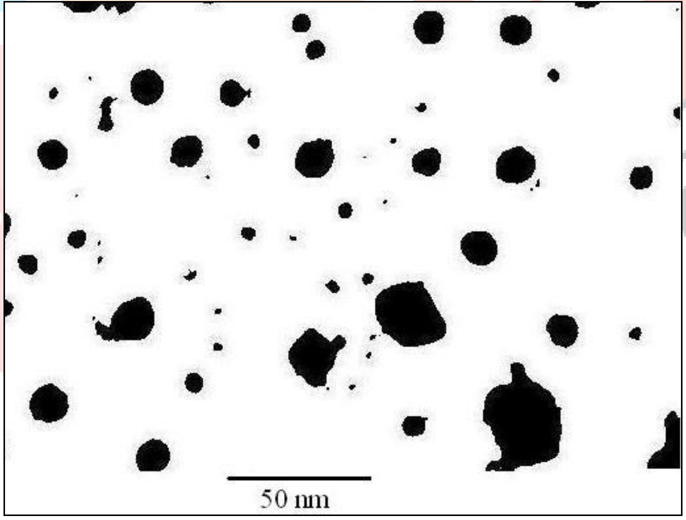

Figure 3 TEM micrograph of the sample S1

We have studied the photoemission behaviour of this ultrafine NiO:Fe system. Fig. 4 shows photoluminescence spectra of the sample at different excitation wavelength. All the patterns show the presence of an intense peak along with two daughter peaks. The existence of the intense peak is attributed to NiO and the small peaks are due to Fe. The two peaks for Fe are observed because of the presence of Fe^{2+} and Fe^{3+}. Due to the dependence of crystal field with excitation energy, the shift is observed for Fe with variation in excitation wavelength. The most intense peak is also showing change in intensity and shift in peak position. As the excitation wavelength increases, the incident laser will be less energetic and hence there will be decrease in the intensity. The shift in the peak position may be attributed to Raman shift. The difference in electro negativity of Ni (1.91) and Fe (1.83) is leading to the formation of different dipoles.

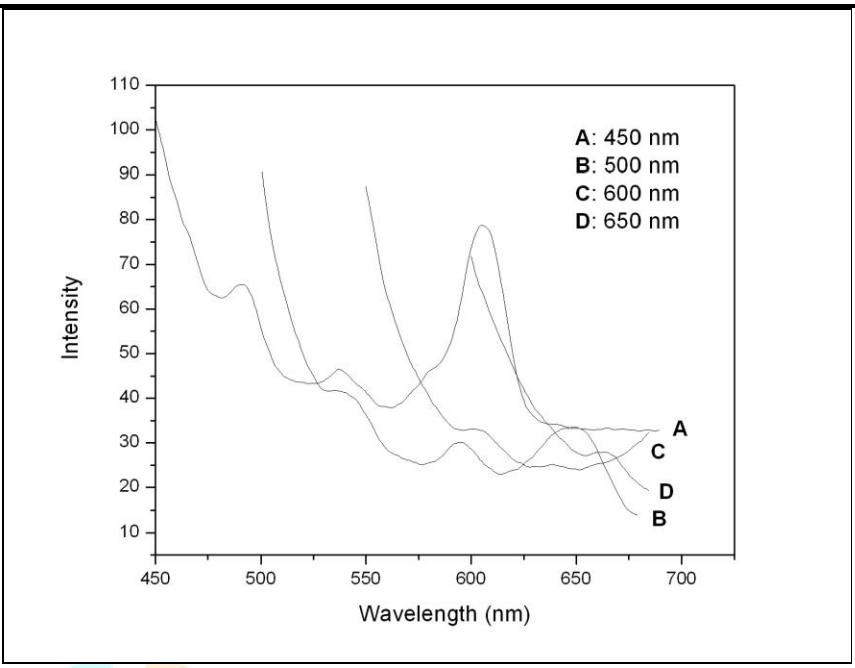

Figure 4 PL spectra of the sample S1

Fig. 5 shows the I-V characteristics of the sample at room temperature. The characteristics curve shows a nonlinear behaviour. The experiment was performed three times to have the reproducibility of datas. The conductivity is found to be $2x10^{-6}$ S/cm. These results strongly indicate the semiconducting behaviour at room temperature of the sample consisting of ultrafine nanoparticles.

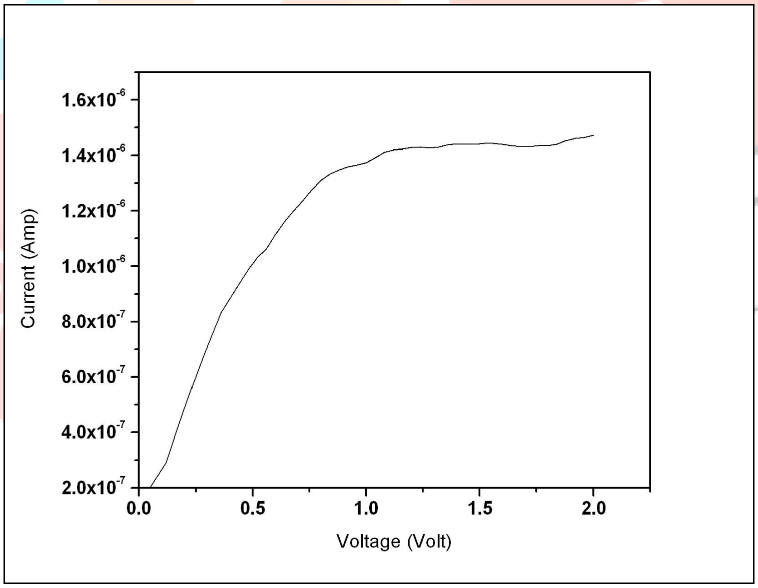

Figure 5 I-V characteristic of the sample S1

To reveal the magnetic behaviour, we characterized the sample with the aid of hysteresis loop tracer at room temperature applying pulsed magnetic fields. Fig. 6 shows the magnetic moment vs. applied magnetic field characteristic of the sample. From the analysis of hysteresis loop, it is found that the saturation magnetization is 1.61 emu/gm at 45 KOe and coercivity is 0.5 KOe. These results indicate the ferromagnetic behaviour of the sample. A detailed study on the magnetic structure and magnetic behaviour at low temperature will enable to understand the physics behind room temperature ferromagnetism in such fine dimension magnetic semiconductor system.

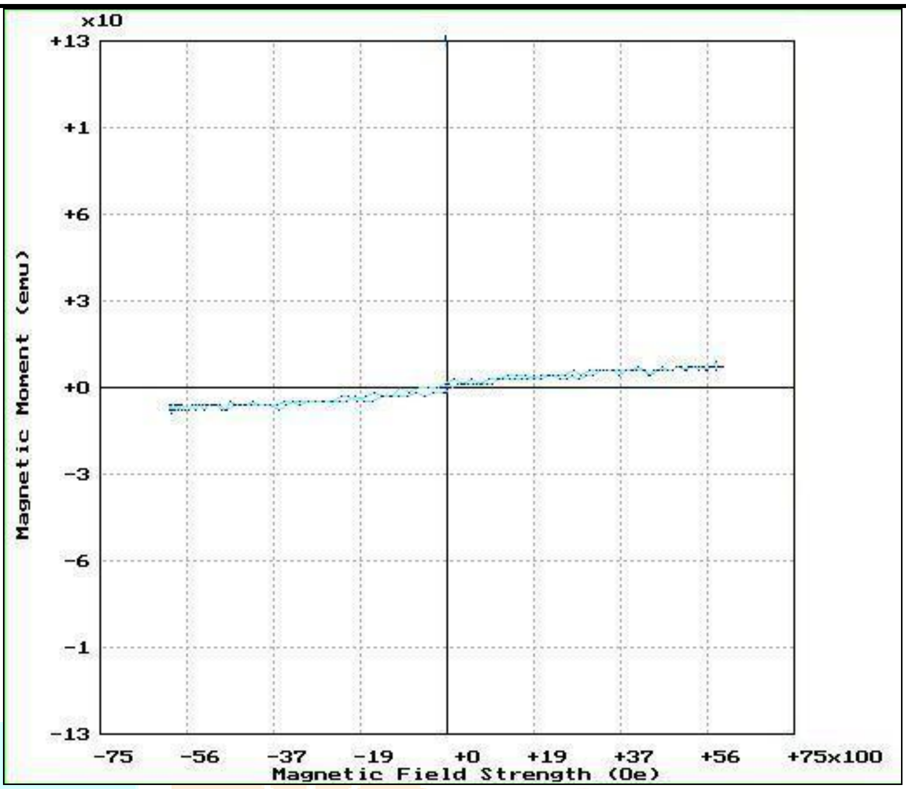

Figure 6 Hysteresis curve of the sample S1

4. Conclusion

In conclusion, polycrstalline single phase NiO:Fe (x=0.04) nanoparticles are prepared. Other co-doped samples with higher doping concentrations are showing presence of several phases of nickel oxide and iron oxide phases and their alloys. The prepared nanoparticle sample is showing ferromagnetic behaviour at room temperature. The semiconducting nature has also been ensured in the sample. The so obtained nanoparticles have spherical dimensions and average particle size 12 nm with a narrow size distribution. The PL spectrum shows the luminescence due to the presence of NiO and doped Fe ions. Raman shift has been observed with the variation in excitation wavelength. Further detailed study on magnetic structure and low temperature magnetic behaviour will shade light on its suitability for spintronics application.

Reference:

1. Xuedong Hu, Rogerio de Sousa, S. Das Sarma, *arXiv:cond-mat/0108339v2*

2. Rogerio de Sousa, S. Das Sarma**,** Phys. Rev. B **67**, 033301 (2003)

3. S. Gardelis, C. G. Smith, C. H. W. Barnes, E. H. Linfield, and D. A. Ritchie, Physical Review B, Volume **60**, Number 11 (1999)

4. B.E. Kane, Nature, **393**, 133 (1998)

5. D. A. Schwartz and D. R. Gamelin, Adv. Mater. (Weinheim, Ger.) **16**,2115 (2004)

6. P. Sharma, A. Gupta, K. V. Rao, F. J. Owens, R. Sharma, R. Ahuja, J. M. Osorio Guillen, B. Johansson, and G. A. Gehring, Nat. Mater. **2**, 673 (2003)

7. T. M. Pekarek and D. J. Arenas, Journal Of Applied Physics Volume **95**, Number 11 (2004)

8. Yuan-Hua Lin, Minghao Ying, Ming Li, Xiaohui Wang, and Ce-Wen Nan, Appl. Phys. Lett. **90**, 222110 (2007)
9. V.G. Storchak, D.G. Eshchenko, H. Luetkens, E. Morenzoni, R.L. Lichti, S.F. Marenkin, O.N. Pashkova, J.H. Brewer, Physica B **374–375**, 430–432 (2006)

10. S. Choi, G. B. Cha, S. C. Hong, S. Cho, Y. Kim, J. B. Ketterson, S. Y. Jeong, and G. C. Yi, Solid State Commun. **122**, 165 (2002)

11. S. A. Chambers, S. Thevuthasan, R. F. C. Farrow, R. F. Marks, J. U. Thiele, L. Folks, M. G. Samant, A. J. Kellock, N. Ruzycki, D. L. Ederer and U. Diebold, Appl. Phys. Lett. **79**, 3476 (2001)

12. Y. Matasumoto, M. Murakami, T. Shono, T. Hesegawa, T. Fukumaura, M. Kawasaki, P. Ahmet, T. Chikyow, S. Koshihara and H. Koinuma, Science, **291**, 854 (2001)

13. K. Sato, P. H. Dederics and H. Katayama-Yoshida, Europhys. Lett., **61** (3), pp. 403–408 (2003)

14. R. J. Powell and W. E. Spicer, Phys. Rev. B **2**, 2182 (1970)

15. L. C. Bartel and B. Morosin, Phys. Rev. B **3**, 1039 (1971)

16. Y. Lin, L. Jiang, R. Zhag, and C. W. Nan, Phys.Rev. B **72**, 014103 (2005)

17. A P Douvalis, L Jankovic and T Bakas, J. Phys.: Condens. Matter **19** 436203 (2007)

18. Yuan-Hua Lin, Jianfei Wang, Jingnan Cai, Minghao Ying, Rongjuan Zhao, Ming Li, and Ce-Wen Nan, Physical Review B **73**, 193308 (2006)

19. J.H. He, S.L. Yuan , Z.M. Tian, Y.S. Yin, P. Li, Y.Q. Wang, K.L. Liu, S.J. Yuan, X.L. Wang, L. Liu, Journal of Magnetism and Magnetic Materials **320**, 3293–3296 (2008)

20. S. Manna, A. K. Deb, J. Jagannath, and S. K. De, J. Phys. Chem. C**, 112**, 10659–10662 (2008)

21. Jianfei Wang, Jingan Cai, Yuan-Hua Lin, and Ce-Wen Nan, Applied Physics Lett. **87**, 202501 (2005)

22. Tanabe. Y, Sugano. S, J. Phys. Soc. Jpn. **9**, 753 (1954)

23. Solomon. E. I., Lever. A. B. P., Eds. *Inorganic Electronic Structure and Spectroscopy*,(John Wiley and Sons, Inc., New York, 1999), Volume 1

Figure Captions:

1. XRD pattern of $Ni_{1-x}Fe_xO$ (x=0.04) sample (S1).
2. XRD pattern of $Ni_{1-x}Fe_xO$ (x=0.2) sample (S2).
3. TEM micrograph of the sample S1.
4. PL spectra of the sample S1.
5. I-V characteristic of the sample S1.
6. Hysteresis curve of the sample S1.

IJCRT

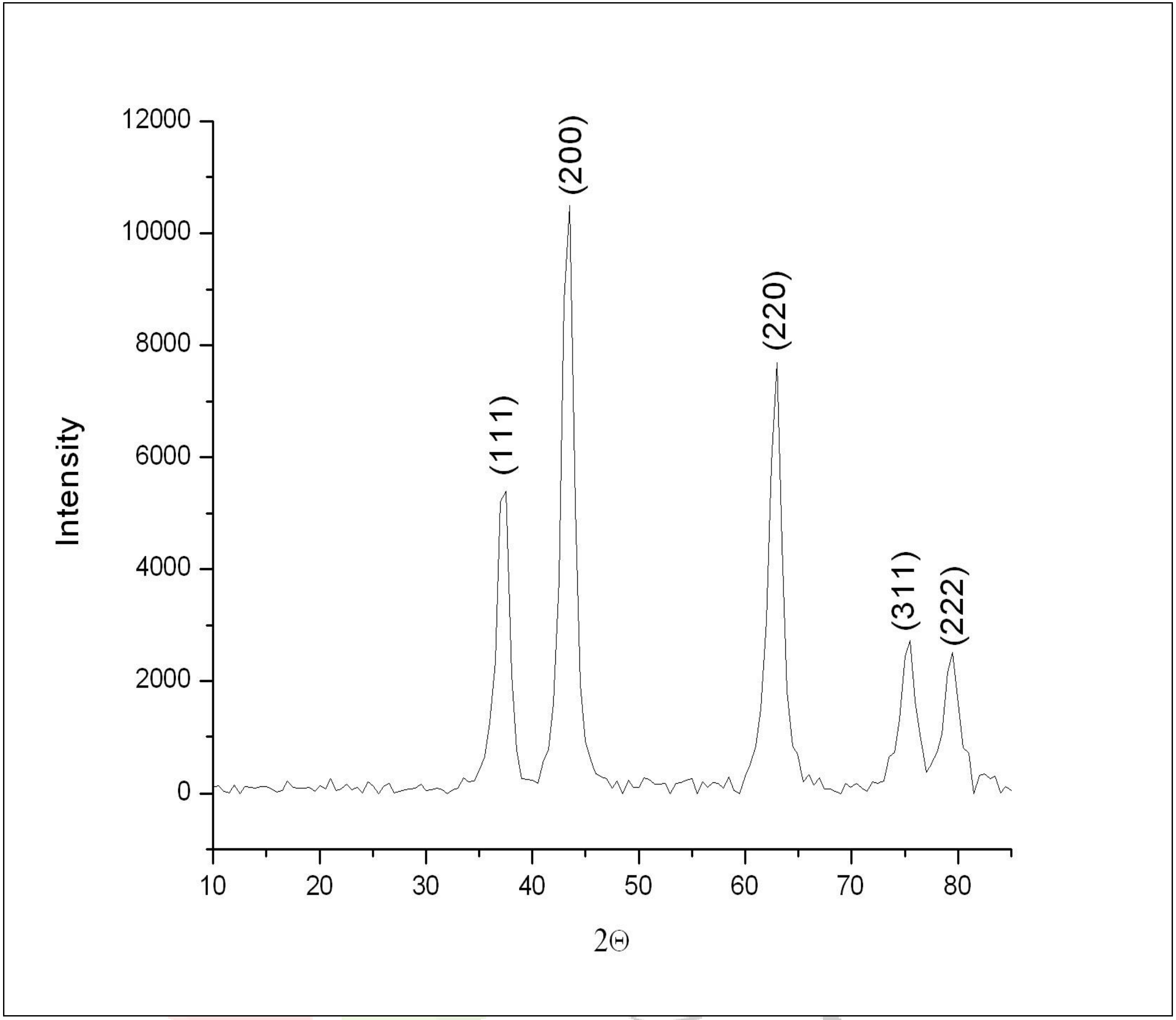

Figure 1 XRD pattern of Ni1-xFexO (x=0.04) sample S1

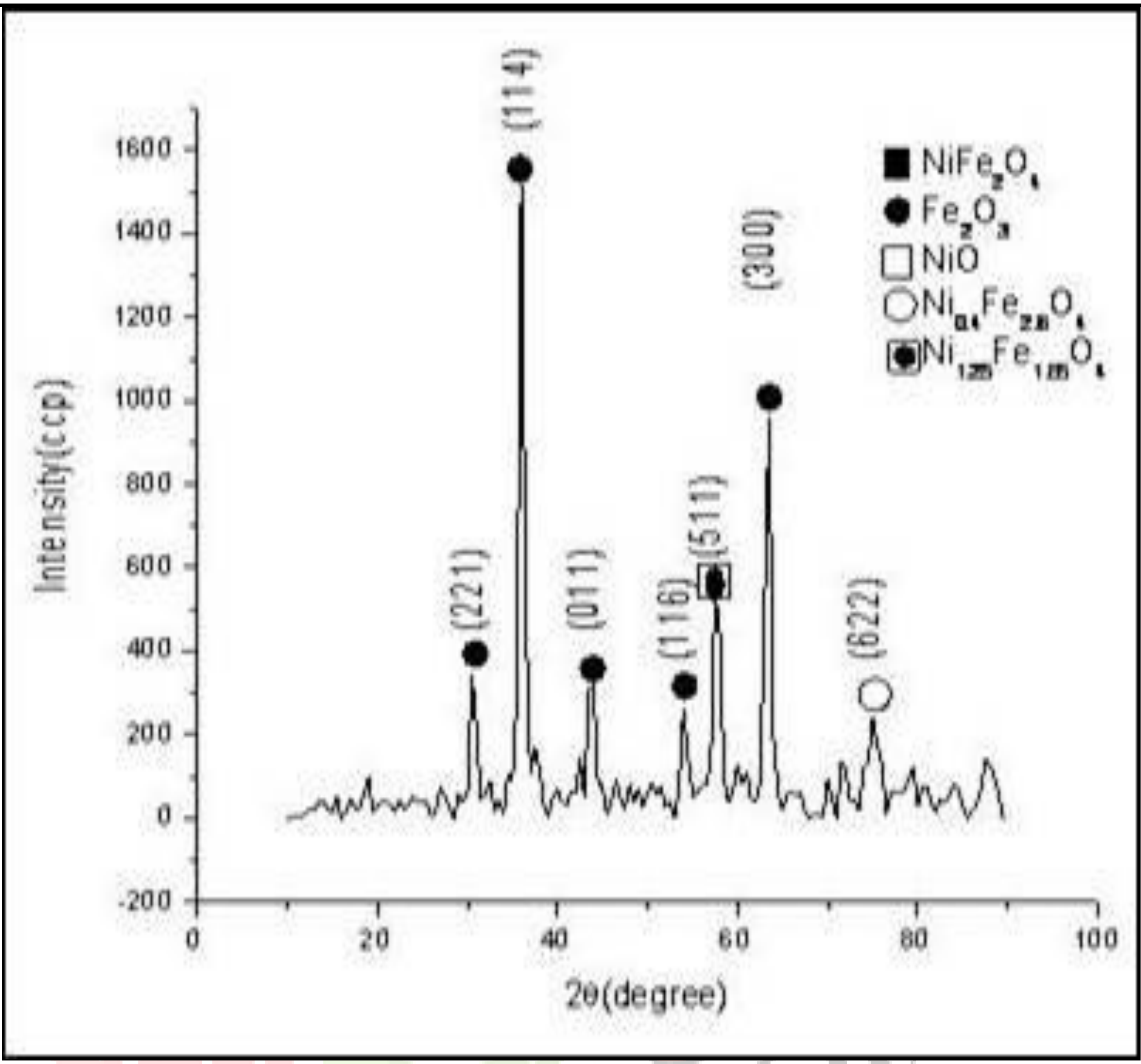

Figure 2 XRD pattern of Ni1-xFexO (x=0.2) sample S2

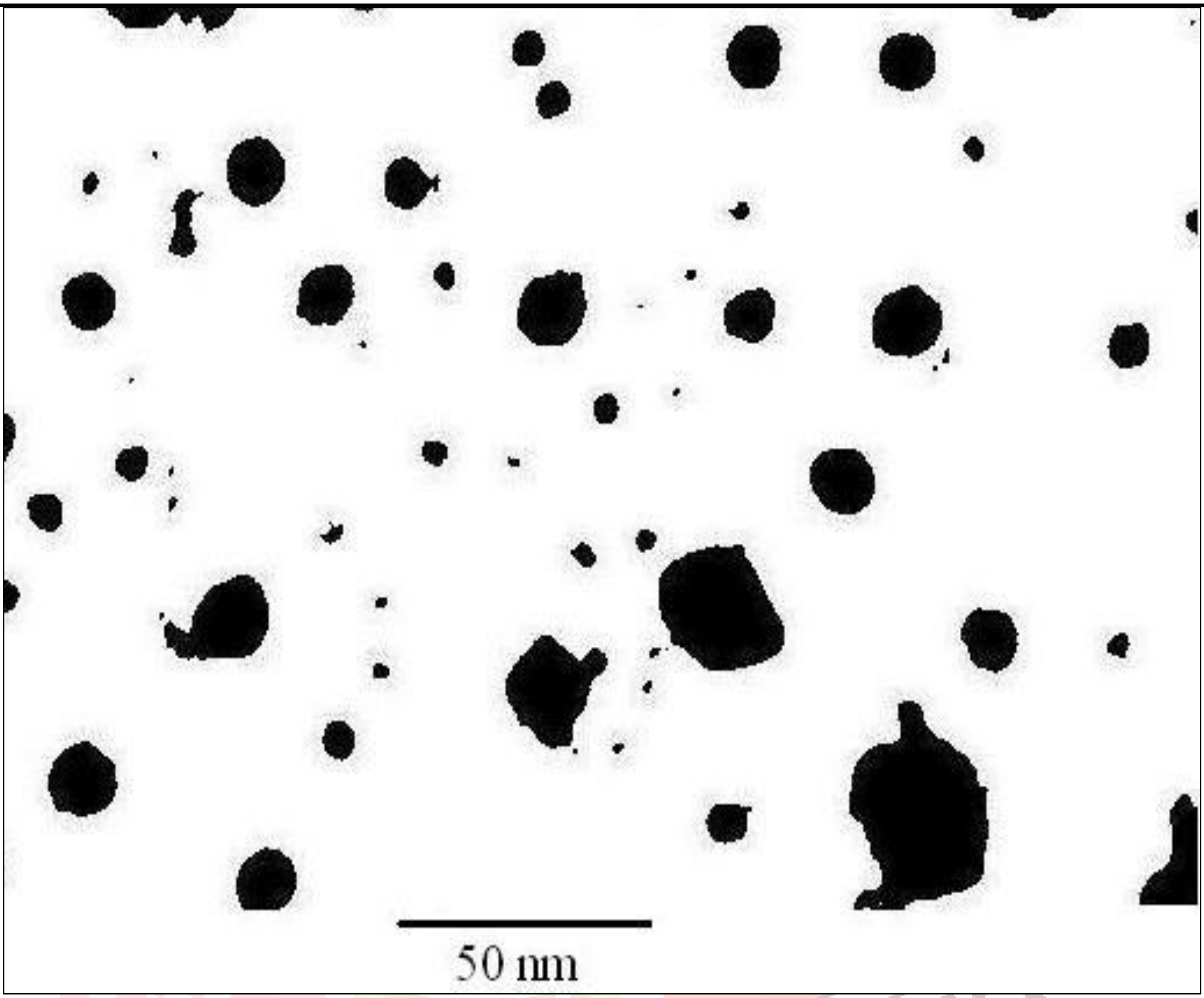

Figure 3 TEM micrograph of the sample S1

IJCRT

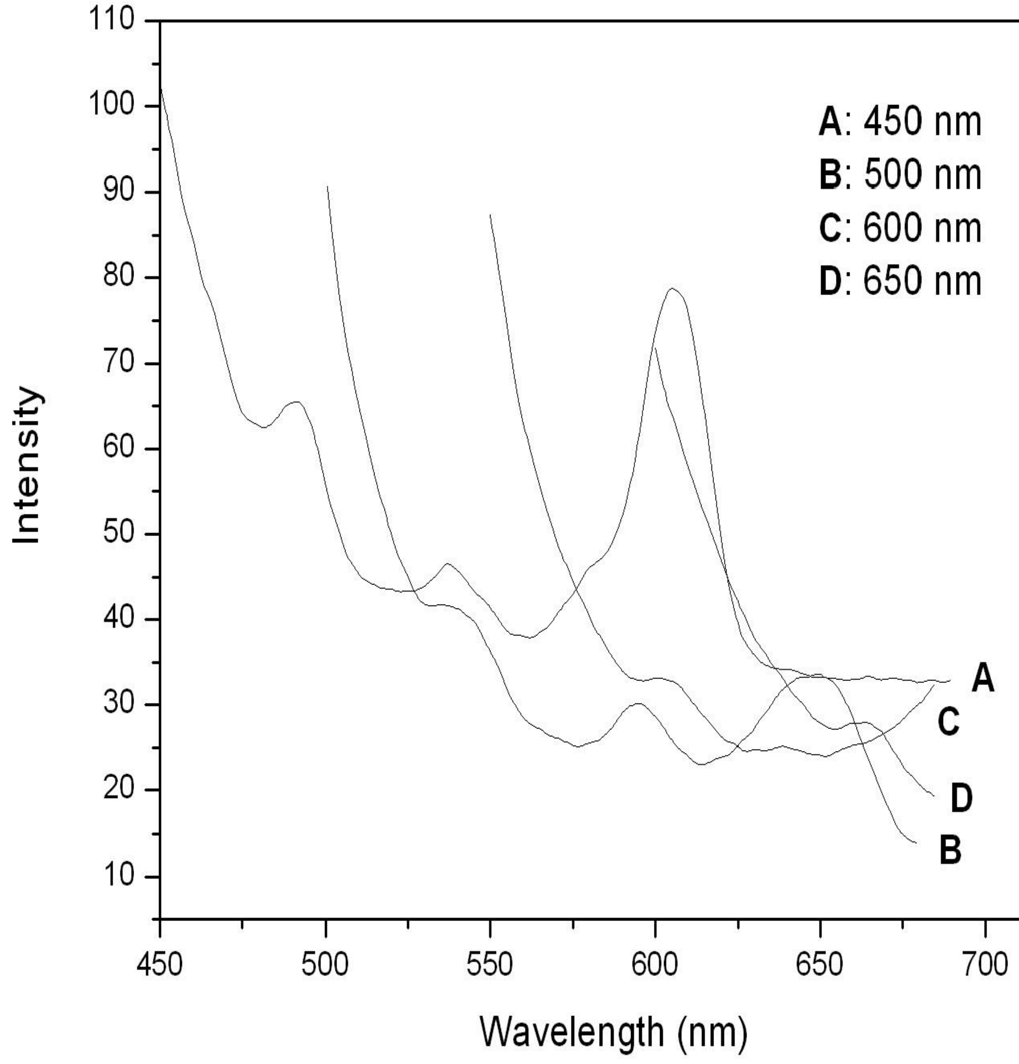

Figure 4 PL spectra of the sample S1

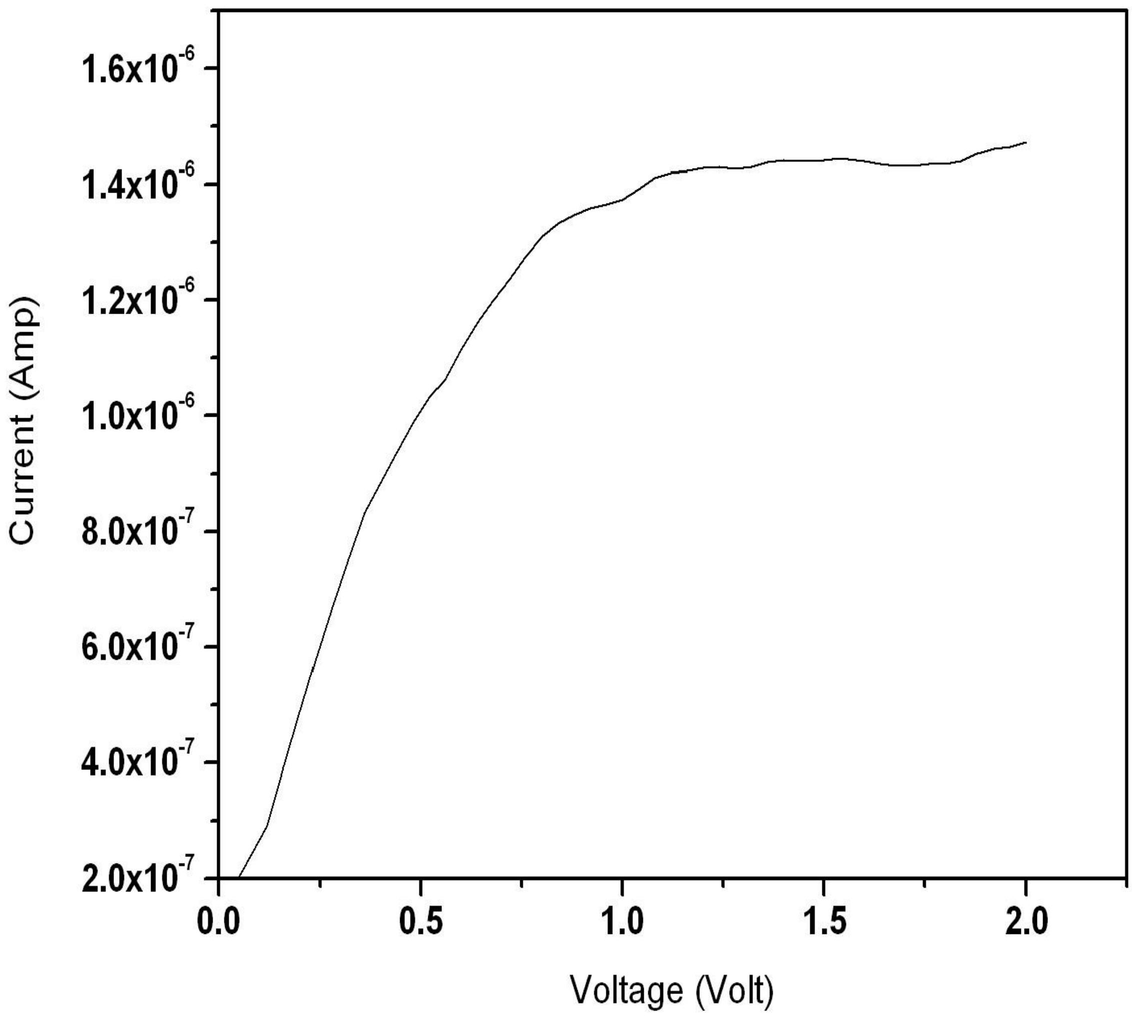

Figure 5 I-V characteristic of the sample S1

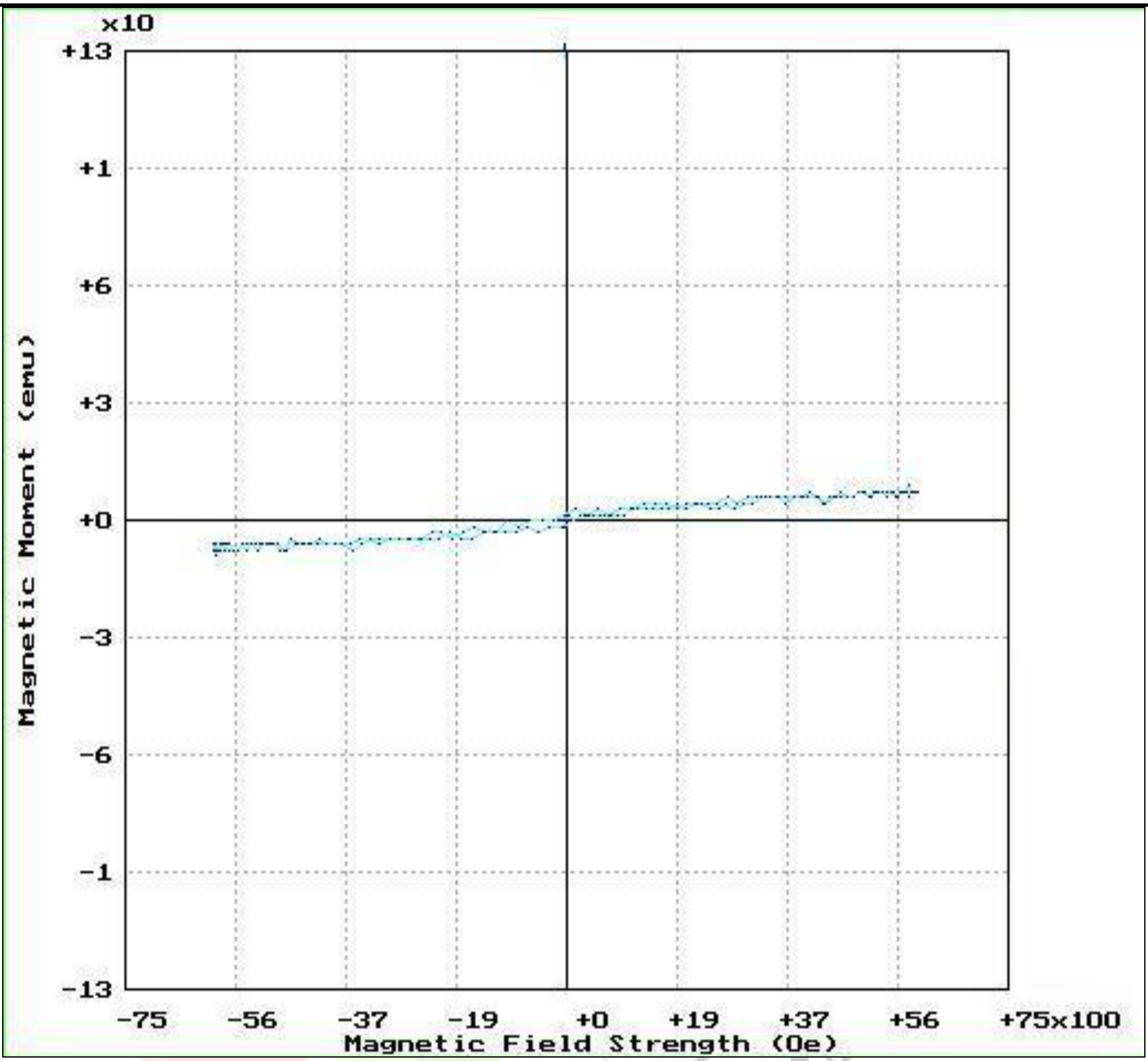

Figure 6 Hysteresis curve of the sample S1